Journal of Engineering and Technology

T-S CONTROLLERS FOR PHOTOVOLTAIC-GRID CONNECTED SYSTEM THROUGH DC-DC BOOST CONVERTER AND THREE PHASE INVERTER

H. Khabou Rekik [1*], M. Souissi [1]

[1]Electrical department, University of Sfax,
National Engineering School of Sfax(ENIS), Laboratory of Sciences and Techniques of Automatic and Industrial Informatic (Lab-STA),
LR11ES50, 3038, Sfax, Tunisia

ABSTRACT

This document presents two on-line T-S fuzzy controllers for controlling the optimal power extraction and its transfer from the PV system through two statics converters into the public network. The first controller is applied on the boost converter to calculate, at every moment, the duty cycle allowing to track the panel maximum power point under climatic variations and achieve a high-efficiency for solar energy harvesting. While the second one adjusts the switching states of the two-level three phase inverter's branches transistors for maximum transfer of the active power produced by the panel to the distribution network with reactive power compensation while establishing synchronization. After grid-connection system structure presentation and mathematic modeling of the converters on the PV-side and the grid-side, the T-S fuzzy controllers are detailed. These controller's synthesis is based on the state space subdivision of the nonlinear system to be controlled into a set of linear subsystems. To ensure the disturbances rejection and guarantee the fuzzy controller's stability, H_∞ criterion and Lyapunov's quadratic stability function are considered. The controller's gains are computed by using the linear matrix inequality (LMI) solution. The numerical simulation results on the Matlab-Simulink environment show the effectiveness and the performances of the proposed controllers.

KEYWORDS: *Grid-connected photovoltaic systems, Takagi-Sugeno (T-S) fuzzy Controller, Maximum Power Point Tracking (MPPT), Linear Matrix Inequality (LMI), Pulse Width Modulation (PWM).*

1.0 INTRODUCTION

Grid-connected photovoltaic systems make up the largest part of PV installations in the world. They have become more popular than stand-alone systems because they do not need storage batteries and therefore less expensive (Rana, M. M., Ali, R. M., Ajad, A. K., & Moznuzzaman, M., 2016). Despite their popularity, this type of power generation system still has some challenges, mainly, the maximum power point tracking (MPPT) algorithm and the control strategy to inject a sinusoidal current into the grid.

Nevertheless, the voltage generated from the PV array is continuous and very low. Thus, the PV generator must be connected to the utility grid through a boost converter to increase the power and an inverter to convert the continuous PV outputs into AC signals. The photovoltaic cells absorb and transform the light rays to produce a low

* Corresponding Email:hajerkhabou@yahoo.fr / hajer.khabou@ipeis.usf.tn

electric current. Their performances are then influenced by environmental factors. In addition, connected directly to a load, these cells cannot transfer the maximum power produced. The procedure employed to relieve the first challenge consist to insert, at the PV module output, a boost converter with a variable duty ratio generated by a control system.

To track the maximum power point (MPP), several algorithms have been detailed and applied by the researchers. Among the most used, the Perturb and Observation (P&O) algorithm, chosen for its simplicity and the reduced cost of its implementation (Hamrouni, N., Jraidi, M., Dhouib, A., & Cherif, A., 2017; Cen, Z., 2017; Bouhafs, A. Lokmane, B. M., & Mohamed, D., 2015; Afkar, H., Shamsinejad, M. A., & Ebadian, M., 2016) and the Incremental Conductance (Refaat, A., Kalas, A., Daoud, A., & Bendary, F., 2013) which improves the P&O results.

Recently, intelligent methods, such as the fuzzy logic-based methods, have invaded the field of MPP research due to their better performance than conventional methods. The Fuzzy Logic Controller (FLC) of Mamdani is frequently used (Yuanlong, L., & Ji, Z., 2018; Srivastava, M., & Saxena, A., 2016; Salah, C. B., & Ouali, M., 2011; Sakthitharani, S., Sangeetha, R., Subha, S., & Deivamani, G., 2018; Mahfouz, M. M., 2018; Cheng, P. C., Peng, B. R., Liu, Y. H., Cheng, Y. S., & Huang, J. W., 2015) but its major disadvantage is that the performance depends on the chosen rules.

The T-S fuzzy model based control becomes also a popular and effective method (Sekhar, P. C., & Mishra, S., 2014; Kumar, A., Vempati, S. A., & Behera, L., A. V., 2013; Chiu, C. S., 2010; Belattar, A., Chennanni, M., & Doubabi, S., 2015; Ajaamoum, M., Kourchi, M., Bouachrine, B., & Ihlal, A., & Bouhouch, L., 2015) mostly for controlling complex nonlinear systems. Comparative studies of the T-S method with other methods (Ounnas, D., Ramdani, M., & Chenikher, S., & Bouktir, T., 2017; Eugineraj, K., & Uma, G., 2013) show superior performance by reducing the oscillations around the MPP and increasing the dynamic response rapidity regardless of the rapid variations in irradiance and temperature values. Moreover, this technique doesn't require precise knowledge of system parameters to achieve better control performance.

As the current-voltage characteristics generated by the PV panel are non-linear, the selected MPPT controller is the T-S fuzzy controller with a strict analysis of stability and performance.

The second challenge of grid-connected solar photovoltaic systems is to attain an optimal PV panel compatibility with the same characteristics of the public network. Typically, a DC-AC converter is the PV interface used to convert the DC current produced by the panel into synchronized sinusoidal waveform with the grid. Furthermore, to achieve the PV generated power and perform the power quality at grid-connected point, different control schemes are developed in the literature to further reduce the current network harmonics and increase the system robustness ahead perturbations.

Although the PI controller has been widely used to control three-phase grid-connected PV systems (Rana, M. M., Ali, R. M., Ajad, A. K., & Moznuzzaman, M., 2016; Hamrouni, N., Jraidi, M., Dhouib, A., & Cherif, A., 2017), its main disadvantage is that

it cannot guarantee the desired control performance in the presence of climatic variations. In addition, the injected current contains some high frequency harmonics. To solve these mentioned problems without specific mathematical models, a T-S fuzzy controller is designed (Gupta, S., Garg, R., & Singh, A., 2015). This controller possesses the ability to approximate non-linear systems and meet with environmental changes.

To properly control the output signals of the three-phase inverter employed to connect the PV system to the grid while reducing harmonic distortion produced by the presence of electronic power interface, the sinusoidal pulse width modulation (SPWM) technique is used.

The remainder of this work is organized as follows: a photovoltaic energy conversion system using a two-level three phase inverter is represented in section 2. In the same section, elementary and global models, PV-side and grid-side, are also developed. The third part deals with control schemes designed around the DC-DC and DC-AC converters. Command strategy and augmented systems are detailed in the sections 4 and 5. Simulation results are represented and discussed in Section 6. Finally, the conclusion is presented in Section 7.

2.0 PROPOSED SYSTEM STRUCTURE

The configuration of two-levels three phase inverter grid-connected photovoltaic system is shown in Figure 1.

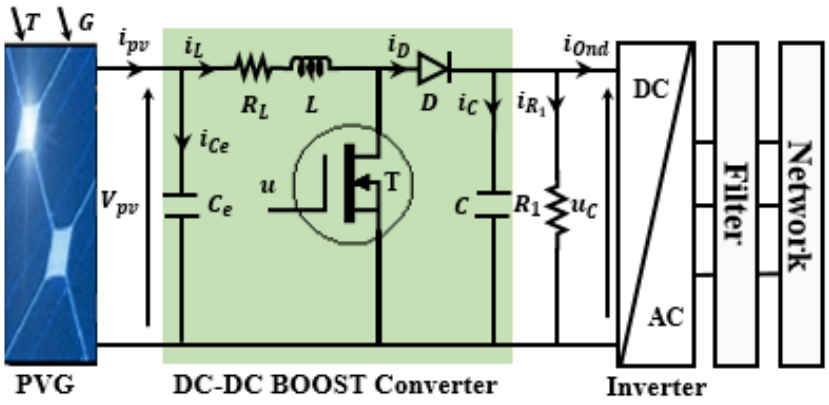

Figure 1. Electrical conversion chain

The study system topology comprises two conversion stages in cascade allowing to transfer the optimal energy extracted from the photovoltaic panel to the utility grid. The first stage, called continuous stage, consists of a photovoltaic generator followed by a DC-DC boost converter used to achieve the maximum power point and boosted the optimal voltage generated to reach a suitable DC bus voltage. The second one or the alternative stage type is made up of two-levels three phase DC-AC inverter and an inductive filter coupled to the electrical network.

According to the literature, the best-known PV cells equivalent circuit model is the cell basic model consisted of an ideal current generator mounted in parallel with a single diode and shunt resistance, which represents the leakage current, related in series with a

series resistance to symbolizes the internal resistance (Yahya, A. O. M., Mahmoud, A. O., & Issakha, Y., 2008). Since the value of the shunt resistor is too large compared to the series resistance (Abada, S., & Lehuy, H., 2011), the current cross through it can be neglected.

This structure enables the continuous and uninterrupted exchange of energy between a photovoltaic installation and the electricity grid. The mathematical models of PV-boost and inverter-filter-grid coupling will be presented in the next section.

2.1 Pv-Side Converter Modelization

The climatic conditions variation generates instantaneous fluctuations of the optimal PV power. Therefore, in order to ensure optimum extraction of PV power and increase the panel output voltage, it is essential to consider a DC-DC boost converter. This elevator converter produces an output voltage (u_c) greater than its input voltage (V_{pv}) leading to a current (i_D) lower than the input current (i_L).

Based on Figure 1 and neglecting the i_{Ce} current ($i_{pv}(t) \approx i_L(t)$), the dynamical behavior of the PV-side converter can be approximated by the following set of differential equations:

$$\begin{cases} \dfrac{di_L(t)}{dt} = -\dfrac{R_L}{L} i_L(t) - \dfrac{1}{L} u_c(t) + \dfrac{u_c(t)}{L} u_1 + \dfrac{1}{L} V_{pv}(t) \\ \dfrac{du_c(t)}{dt} = \dfrac{1}{C} i_L(t) - \dfrac{i_{Ond}}{C u_c} u_c(t) - \dfrac{i_L(t)}{C} u_1 - \dfrac{1}{C R_1} u_c(t) \end{cases} \quad (1)$$

where: i_L, u_c, i_{Ond} and V_{pv} design respectively the inductance current, the DC bus voltage, the inverter current, and the PVG voltage.

R_L is the inductance resistance and u_1 is the converter duty cycle, $u_1 \in \{0,1\}$, generated by a pulse width modulator (PWM) scheme whose input signal is emitted by the T-S fuzzy controller. The output voltage (u_c) and the inductor current (i_L) are two power accumulation elements and thus two variables to control.

The state vector corresponding to the set PVG-boost converter is given by:

$$x_1(t) = \begin{bmatrix} i_L(t) & u_c(t) \end{bmatrix}^T \quad (2)$$

$$\dot{x}_1(t) = \begin{bmatrix} \dfrac{di_L(t)}{dt} & \dfrac{du_c(t)}{dt} \end{bmatrix}^T \quad (3)$$

So, the equation (1) can be noted in the following form:

$$\dot{x}_1(t) = A_1(x_1)\, x_1(t) + B_1(x_1)\, u_1(t) + D_1\, h_1(t) \quad (4)$$

$$\text{with } A_1 = \begin{bmatrix} -\frac{R_L}{L} & -\frac{1}{L} \\ \frac{1}{C} & -\frac{i_{Ond}}{Cu_c} \end{bmatrix}, B_1 = \begin{bmatrix} \frac{u_c(t)}{L} \\ -\frac{i_L(t)}{C} \end{bmatrix} \text{ and } D_1 = \begin{bmatrix} \frac{1}{L} & 0 \\ 0 & -\frac{1}{CR_1} \end{bmatrix} \tag{5}$$

The disturbance vector is defined by: $h_1(t) = \begin{bmatrix} V_{pv}(t) & u_c(t) \end{bmatrix}^T$ (6)

The PV generator mathematical model used is deduced from the mono-diode model of the PV cell, where the model inputs are the ambient temperature, the solar irradiance, the PV voltage and the only output is the PV current supplied by the panel. According to the size of the panel, a photovoltaic current can be expressed as:

$$i_{pv} = N_p \left(I_{ph} - I_{rs} \exp\left(\frac{V_{pv}}{N_s V_T} \right) - 1 \right) \tag{7}$$

where I_{rs} and V_T are respectively the reverse saturation current of the diode and the thermal voltage.

The considered photovoltaic generator (PVG) consists of two branches in parallel (N_p), each branch includes (N_s) cells in series.

The PVG-Boost system operates at its maximum power if

$$\frac{dP}{dV_{pv}} = 0 \text{ where } P = V_{pv} i_{pv} \tag{8}$$

and the considered control output is chosen as follows:

$$y_1(t) = \frac{dP}{dV_{pv}} = C_1(x_1).x_1(t) \tag{9}$$

$$\text{with } C_1 = \begin{bmatrix} 0 & \frac{i_{pv}(t)}{u_c(t)} - \frac{V_{pv}(t)}{u_c(t)} . \frac{N_p I_{rs}}{N_s V_T} \exp\left(\frac{V_{pv}(t)}{N_s V_T} \right) \end{bmatrix} \tag{10}$$

2.1.1. Grid-Side Converter Modelization

Among all the existing converter topologies, it is affirmed that multilevel converters represent one of the most important appearances in particular the three-phase converter, (Kouro, J., Leon, I. J., Vinnikov, D., & Franquelo, G. L., 2015; Akoro, E., Amadou, S. M., & Jean-Philippe, T. G., F, 2017). It is a topology widely used in many fields of application, including electrical systems using renewable energies. The DC-AC converter is utilized to convert the voltage from DC to three-phase AC (Cen, Z., 2017). The used converter consists of three branches, each containing two complementary switching cells. Each switch is formed of an ideal transistor and an antiparallel diode

allowing current to flow in both directions. To avoid shorting, both inverter leg switches are never active at the same time.

The mathematical expressions between the diode output current (Figure 1), the currents which pass through the resistance and capacitor and the injected current to the inverter , enable to describe the system by the following model :

$$\begin{cases} \dfrac{di_{od}}{dt} = -\dfrac{R_f}{L_f} i_{od} + w i_{oq} - \dfrac{u_c}{2L_f}\beta_{od} + \dfrac{1}{L_f} V_{rd} \\ \dfrac{di_{oq}}{dt} = -w i_{od} - \dfrac{R_f}{L_f} i_{oq} - \dfrac{u_c}{2L_f}\beta_{oq} + \dfrac{1}{L_f} V_{rq} \\ \dfrac{du_c}{dt} = \dfrac{3}{4C}\beta_{od} i_{od} + \dfrac{3}{4C}\beta_{oq} i_{oq} + \left(\dfrac{i_{pvm}}{Cu_c} - \dfrac{1}{RC}\right) u_c - \dfrac{1}{C} i_{pv1} \end{cases} \quad (11)$$

with $i_D = i_{pvm} + i_{pv1}$ to consider i_{pv1} as a perturbation, $(i_{od}(t), i_{oq}(t))$ are the direct and quadratic components inverter currents and $(V_{rd}(t), V_{rq}(t))$ are the direct and quadratic components grid voltages. These components are calculated using the park transformation applied respectively to the network currents $(i_a(t), i_b(t), i_c(t))$ and the network voltages $(v_a(t), v_b(t), v_c(t))$.

$\beta_{od}(t)$ and $\beta_{oq}(t)$ are the direct and the quadratic components of the inverter laws (S_a, S_b, S_c) calculated with T-S controller.

R_f and L_f are respectively the resistance and the inductance of the filter and w is the angular electric speed.

To model the coupling between the three-phase inverter and the network, the state vector used and the control law are defined by the following expressions:

$$x_2(t) = \begin{bmatrix} i_{od}(t) & i_{oq}(t) & u_c(t) \end{bmatrix}^T \text{ and } u_2(t) = \begin{bmatrix} \beta_{od}(t) & \beta_{oq}(t) \end{bmatrix}^T \quad (12)$$

$$\text{Noting} \quad \dot{x}_2(t) = \begin{bmatrix} \dfrac{di_{od}(t)}{dt} & \dfrac{di_{oq}(t)}{dt} & \dfrac{du_c(t)}{dt} \end{bmatrix}^T \quad (13)$$

Thus, the model of the inverter coupled with the grid (eq. (11)) can be put in the following matrix form:

$$\dot{x}_2(t) = A_2(x_2).x_2(t) + B_2(x_2).u_2(t) + D_2.h_2(t) \quad (14)$$

$$\text{where } A_2 = \begin{bmatrix} -\frac{R_f}{L_f} & w & 0 \\ -w & -\frac{R_f}{L_f} & 0 \\ -\frac{3}{4C}\beta_{od}(t) & -\frac{3}{4C}\beta_{oq}(t) & \frac{i_{pvm}}{Cu_c} - \frac{1}{RC} \end{bmatrix},$$

$$B_2 = \begin{bmatrix} -\frac{u_c(t)}{2L_f} & 0 \\ 0 & -\frac{u_c(t)}{2L_f} \\ 0 & 0 \end{bmatrix} \text{ and } D_2 = \begin{bmatrix} \frac{1}{L_f} & 0 & 0 \\ 0 & \frac{1}{L_f} & 0 \\ 0 & 0 & -\frac{1}{C} \end{bmatrix} \quad (15)$$

with $i_{pv1} = \frac{i_{pvm}}{2}$ and the disturbance vector is expressed as:

$$h_2(t) = \begin{bmatrix} V_{rd}(t) & V_{rq}(t) & i_{pv1}(t) \end{bmatrix}^T \quad (16)$$

In order to accomplish the desired objectives, the design of the TS fuzzy controllers applied to both converters will be detailed later.

3.0 DESIGN OF THE PROPOSED CONTROLLERS

In this section, the command approaches enable to pilot the two statics converters used in PV-side and grid-side are detailed. These commands allow to maximize the panel production to increase the optimal power regardless of climatic factors.

The proposed control system consists mainly of two control blocks: The first block control applies the MPPT algorithm based on T-S fuzzy model on the DC/DC boost converter connected with the photovoltaic panel to extract the maximum power under variable environmental conditions. The second one commands the inverter on the grid-side enables to inject the optimal power extracted into the distribution network while controlling the active and reactive powers. It also allows to maintain the DC bus voltage constant.

3.1 Photovoltaic Source Side Control

As mentioned in Figure 2, a MPPT controller is applied to the boost converter allowing to track, in a continuous way, the MPP to an efficient use of this PV source.

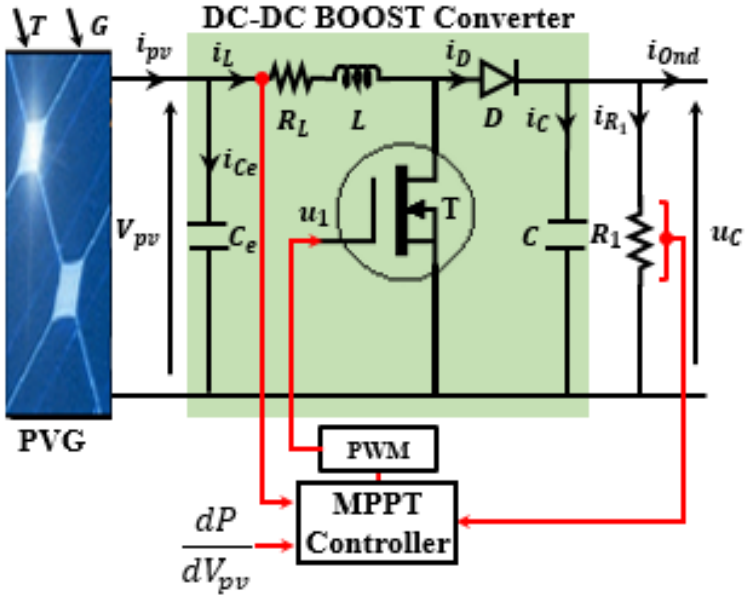

Figure 2. BOOST controller

This algorithm calculates and adapts the duty cycle « u_1 » which will be applied into MOSFET switch of boost converter after generating PWM. This command allows the panel to operate at the maximum power point (MPP) guaranteeing the extraction of the optimal power.

The equations (1) and (7) describing the PVG-Boost system are nonlinear. Therefore, and in order to transform the non-linear model into a linear model, the T-S method fuzzy premise variables are chosen as follows:

$$q_{11} = u_c(t),\ q_{12} = i_L(t),\ q_{13} = \frac{i_L(t)}{u_c(t)}\ and\ \ q_{14} = \frac{V_{pv}(t)}{u_c(t)}.\frac{N_p I_{rs}}{N_s V_T}\exp\left(\frac{V_{pv}(t)}{N_s V_T}\right) \tag{17}$$

The appropriate subsystem matrices are given as:

$$A_{1i} = A_1 = \begin{bmatrix} -\frac{R_L}{L} & -\frac{1}{L} \\ \frac{1}{C} & -\frac{i_{Ond}}{Cu_c} \end{bmatrix}, B_{1i} = \begin{bmatrix} \frac{q_{11i}(t)}{L} \\ -\frac{q_{12i}(t)}{C} \end{bmatrix}, D_{1i} = D_1 = \begin{bmatrix} \frac{1}{L} & 0 \\ 0 & -\frac{1}{CR_1} \end{bmatrix} \text{ and } C_{1i} = \begin{bmatrix} 0 & q_{13i} - q_{14i} \end{bmatrix}$$

(18)

The T-S fuzzy rules can be expressed as follows:

If $q_{11}(t)$ is F_{11i} and $\ldots q_{14}(t)$ is F_{14i},

$$\text{then} \quad \begin{cases} \dot{x}_1(t) = A_{1i}(x_1).x_1(t) + B_{1i}(x_1).u_1(t) + D_{1i}(x_1).h_1(t) \\ y_1(t) = C_{1i}(x_1).x_1(t) \qquad\qquad with\ i = 1,2,\ldots,16 \end{cases} \tag{19}$$

where F_{1ji} are the fuzzy sets.

The T-S fuzzy system overall model is denoted as follows:

$$\begin{cases} \dot{x}_1(t) = \sum_{i=1}^{16} \mu_{1i}\left(q_1(t)\right)\left\{A_{1i}x_1(t) + B_{1i}u_1(t) + D_{1i}h_1(t)\right\} \\ y_1(t) = \sum_{i=1}^{16} \mu_{1i}\left(q_1(t)\right)C_{1i}.x_1(t) \qquad with\ i = 1,2,...,16 \end{cases} \tag{20}$$

The variables premise vector $q_{1}(t)$ is defined by:

$$q_1(t) = \left[\, q_{11}(t) \quad q_{12}(t) \quad q_{13}(t) \quad q_{14}(t) \,\right]^T \tag{21}$$

$\mu_i(q_1(t))$ is the activation degree for each rule *i* represented by the following normalized form:

$$\mu_{1i}\left(q_1(t)\right) = \frac{w_{1i}\left(q_1(t)\right)}{\sum_{i=1}^{16} w_{1i}\left(q_1(t)\right)} \tag{22}$$

for all t, it is given : $w_{1i}\left(q_1(t)\right) = \prod_{j=1}^{4} F_{1ji}\left(q_1(t)\right) and \sum_{i=1}^{16} \mu_{1i}\left(q_1(t)\right) = 1$ (23)

The general form of the membership functions is given by:

$$f_{a1j} = \frac{q_{1j}(t) - qm_{1j}}{qM_{1j} - qm_{1j}}\ and\ f_{b1j} = 1 - f_{a1j} \tag{24}$$

where qM_{1j} and qm_{1j} are the upper and the lower bounds of the variable $q_{1j}(t)$ for j=1, 2, 3, 4.

Table 1 represents the 16 Fuzzy rules form.

Table 1. Fuzzy rules from 1 To16

Fuzzy sets of rules				***Parameters of then-part***			
$\boldsymbol{F_{11i}}$	$\boldsymbol{F_{12i}}$	$\boldsymbol{F_{13i}}$	$\boldsymbol{F_{14i}}$	$\boldsymbol{q_{11i}}$	$\boldsymbol{q_{12i}}$	$\boldsymbol{q_{13i}}$	$\boldsymbol{q_{14i}}$
f_{a11}	f_{a12}	f_{a13}	f_{a14}	qM_{11}	qM_{12}	qM_{13}	qM_{14}
f_{a11}	f_{a12}	f_{a13}	f_{b14}	qM_{11}	qM_{12}	qM_{13}	qm_{14}
f_{a11}	f_{a12}	f_{b13}	f_{a14}	qM_{11}	qM_{12}	qm_{13}	qM_{14}
f_{a11}	f_{a12}	f_{b13}	f_{b14}	qM_{11}	qM_{12}	qm_{13}	qm_{14}
f_{a11}	f_{b12}	f_{a13}	f_{a14}	qM_{11}	qm_{12}	qM_{13}	qM_{14}
f_{a11}	f_{b12}	f_{a13}	f_{b14}	qM_{11}	qm_{12}	qM_{13}	qm_{14}
f_{a11}	f_{b12}	f_{b13}	f_{a14}	qM_{11}	qm_{12}	qm_{13}	qM_{14}
f_{a11}	f_{b12}	f_{b13}	f_{b14}	qM_{11}	qm_{12}	qm_{13}	qm_{14}
f_{b11}	f_{a12}	f_{a13}	f_{a14}	qm_{11}	qM_{12}	qM_{13}	qM_{14}

f_{b11}	f_{a12}	f_{a13}	f_{b14}	qm_{11}	qM_{12}	qM_{13}	qm_{14}
f_{b11}	f_{a12}	f_{b13}	f_{a14}	qm_{11}	qM_{12}	qm_{13}	qM_{14}
f_{b11}	f_{a12}	f_{b13}	f_{b14}	qm_{11}	qM_{12}	qm_{13}	qm_{14}
f_{b11}	f_{b12}	f_{a13}	f_{a14}	qm_{1}	qm_{12}	qM_{13}	qM_{14}
f_{b11}	f_{b12}	f_{a13}	f_{b14}	qm_{11}	qm_{12}	qM_{13}	qm_{14}
f_{b11}	f_{b12}	f_{b13}	f_{a14}	qm_{11}	qm_{12}	qm_{13}	qM_{14}
f_{b11}	f_{b12}	f_{b13}	f_{b14}	qm_{11}	qm_{12}	qm_{13}	qm_{14}

3.2 The Network Side Control

The T-S control method is chosen as the optimum control strategy for the grid inverter control. In this subsection, Figure 3 represent the control method detail applied to the inverter. This aims to calculate the inverter command signals (S_a, S_b, S_c) permitting to transfer the maximum energy produced to the network.

Applying the PARK transformation to the inverter current-voltage components and the network voltage components, the T-S controller uses the obtained variables $\left(i_{od}(t), i_{oq}(t), v_{od}(t), v_{oq}(t), V_{rd}(t), V_{rq}(t)\right)$ as an input to calculate the inverter command laws $\left(\beta_{od}(t), \beta_{oq}(t)\right)$.

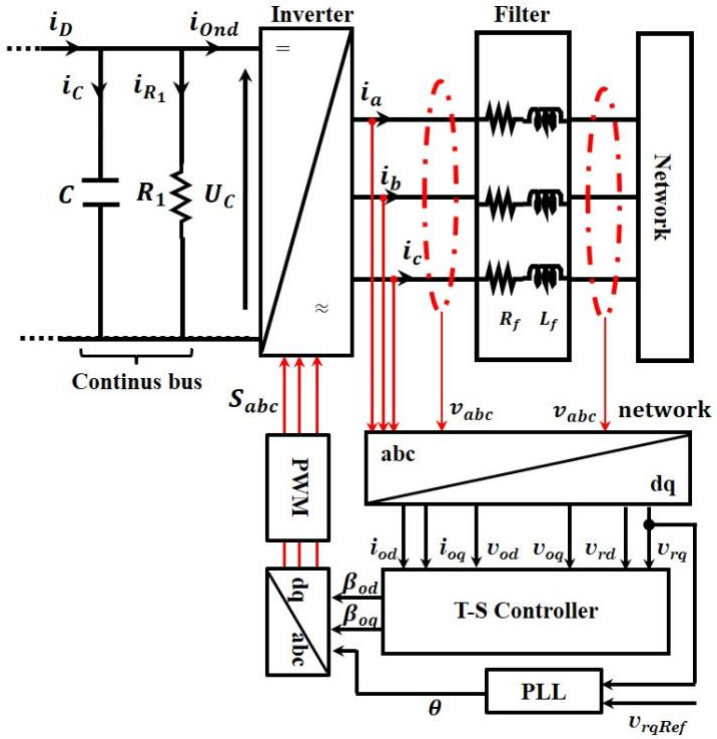

Figure 3 Inverter controller

The network quadratic voltage deduced from PARK transformation as well as its chosen reference value are used as inputs to the Phase Lock Loop (PLL) module (Figure 4) to generate the angle phase θ.

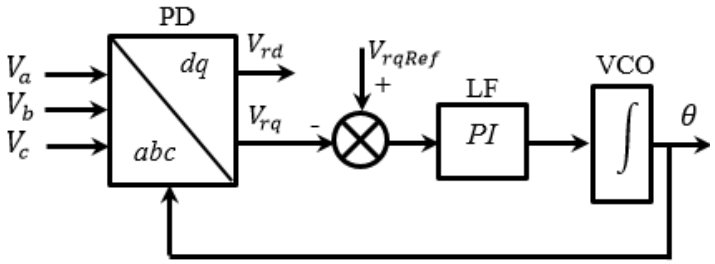

Figure 4. Basic scheme of a conventional PLL

To calculate the switches commands of the three branches of the inverter, the reverse PARK transform is applied on the d-q command laws using the calculated phase angle. After that, to control the instantaneous current waveform with high accuracy while reducing the Total Harmonic Distortion (THD) and the harmonic noise, the sinusoidal Pulse Width Modulation (PWM) is used (Bouhafs, A. Lokmane, B. M., & Mohamed, D., 2015) to generate the switching states (S_a, S_b, S_c) of the three inverter branches.

The inverter output signals are then filtered to supply the network with quasi-sinusoidal waveform currents.

The non-linearity of the mathematical model (eq. (15)) requires the use of the T-S controller whose premises variables are chosen as follows:

$$q_{21}(t) = \beta_{od}(t), q_{22}(t) = \beta_{oq}(t) \; and, q_{23}(t) = u_c(t) \tag{25}$$

$$\text{So} \qquad q_2(t) = \begin{bmatrix} q_{21}(t) & q_{22}(t) & q_{23}(t) \end{bmatrix} \tag{26}$$

Thus, the nonlinear inverter system can be described by a set of 2_3 fuzzy T-S rules represented in the form:

If $q_{21}(t)$ is F_{21i}, $q_{22}(t)$ is F_{22i} and $q_{23}(t)$ is F_{23i},

$$\text{then } \dot{x}_2(t) = A_{2i}\, x_2(t) + B_{2i}\, u_2(t) + D_2\, h_2(t) \tag{27}$$

with $i = 1, \ldots, r_2$ and $F_{2\,ji}$ are the fuzzy sets and r_2 is the fuzzy rules number ($r_2 = 8$).
The overall T-S fuzzy system model can be denoted in the form of a weighted sum as follows:

$$\dot{x}_2(t) = \sum_{i=1}^{8} \mu_{2i}\left(q_2(t)\right)\left\{A_{2i}x_2(t) + B_{2i}u_2(t) + D_{2i}h_2(t)\right\} \tag{28}$$

where matrices A_{2i} and B_{2i} are given by:

$$A_{2i}=\begin{bmatrix} -\frac{R_f}{L_f} & w & 0 \\ -w & -\frac{R_f}{L_f} & 0 \\ -\frac{3q_{21i}}{4C} & -\frac{3q_{22i}}{4C} & \frac{i_{pvm}}{Cu_c}-\frac{1}{R_1C} \end{bmatrix}, B_{2i}=\begin{bmatrix} -\frac{q_{23i}}{2L_f} & 0 \\ 0 & -\frac{q_{23i}}{2L_f} \\ 0 & 0 \end{bmatrix} \quad (29)$$

The activation degree for each rule is represented by the following form:

$$\mu_{2i}\left(q_2(t)\right)=\frac{w_{2i}\left(q_2(t)\right)}{\sum_{i=1}^{8} w_{2i}\left(q_2(t)\right)} \quad (30)$$

$$\text{for all } t:\ w_{2i}\left(q_2(t)\right)=\prod_{j=1}^{3} F_{2ji}\left(q_2(t)\right) \text{ and } \sum_{i=1}^{8}\mu_{2i}\left(q_2(t)\right)=1 \quad (31)$$

The general form of the membership functions is given by:

$$f_{a2j}=\frac{q_{2j}(t)-qm_{2j}}{qM_{2j}-qm_{2j}} \text{ and } f_{b2j}=1-f_{a2j} \quad (32)$$

where qM_{2j} and qm_{2j} are the upper and the lower bounds of the variable $q_{2j}(t)$ for j=1, 2, 3.

The Fuzzy rules form are represented on the Table 2.

Table 2. Fuzzy rules from 1 to 8

Fuzzy sets of rules			***Parameters of then-part***		
$\boldsymbol{F_{21i}}$	$\boldsymbol{F_{22i}}$	$\boldsymbol{F_{23i}}$	$\boldsymbol{q_{21i}}$	$\boldsymbol{q_{22i}}$	$\boldsymbol{q_{23i}}$
f_{a21}	f_{a22}	f_{a23}	qM_{21}	qM_{22}	qM_{23}
f_{a21}	f_{a22}	f_{b23}	qM_{21}	qM_{22}	qm_{23}
f_{a21}	f_{b22}	f_{a23}	qM_{21}	qm_{22}	qM_{23}
f_{a21}	f_{b22}	f_{b23}	qM_{21}	qm_{22}	qm_{23}
f_{b21}	f_{a22}	f_{a23}	qm_{21}	qM_{22}	qM_{23}
f_{b21}	f_{a22}	f_{b23}	qm_{21}	qM_{22}	qm_{23}
f_{b21}	f_{b22}	f_{a23}	qm_{21}	qm_{22}	qM_{23}
f_{b21}	f_{b22}	f_{b23}	qm_{21}	qm_{22}	qm_{23}

4.0 COMMAND STRATEGY

The optimal control strategy chosen to control the used converters must be allowed to extract the maximum power produced by the PV panels and ensure its optimal transfer to the network. This power is represented in two forms active and reactive expressed by:

$$P = V_{rd} i_{od} + V_{rq} i_{oq} \tag{33}$$

$$Q = -V_{rd} i_{oq} + V_{rq} i_{od} \tag{34}$$

As the photovoltaic system generates only the active power; the reactive power can must cancel. To ensure this criterion, two conditions on the quadratic components are imposed and given by the following expressions: $i_{oq\mathrm{Re}f} = 0$ and $V_{rq} = 0$.

To maintain the grid voltage quadratic component to zero, its reference value is imposed equal to zero ($V_{rq\mathrm{Re}f} = 0$). Then, the powers expressions will be denoted by:

$$P = V_{rd} i_{od} \tag{35}$$

$$Q = -V_{rd} i_{oq} = 0 \tag{36}$$

5.0 AUGMENTED SYSTEMS

5.1 Boost Augmented System

The control objective is to regulate the controlled output $y_1(t) = \dfrac{\partial P}{\partial V_{pv}}$ of the photovoltaic array to its

reference value $y_{1\mathrm{Re}f}(t) = \left.\dfrac{\partial P}{\partial V_{pv}}\right|_{MPP} = 0$.

To extract the optimum PV voltage, the T-S fuzzy controller is applied on the first converter to calculate the duty cycle u_1 to command the boost transistor.

The boost augmented vector is noted as follows:

$$\bar{x}_1 = \begin{bmatrix} x_1 & e_{1I} \end{bmatrix}^T \text{ and } \dot{\bar{x}}_1 = \begin{bmatrix} \dot{x}_1 & e_1 \end{bmatrix}^T \tag{37}$$

where the boost error vector is defined by:

$$e_1(t) = y_1(t) - y_{1\mathrm{Re}f}(t) = \frac{\partial p}{\partial V_{pv}} - 0 = C_1\left(x_1(t) - x_{1\mathrm{Re}f}(t)\right) \tag{38}$$

and $e_{1I} = \int e_1$.

So, the boost augmented system can be described by:

$$\dot{\bar{x}}_1(t)=\begin{bmatrix}\sum_{i=1}^{16}\mu_{1i}\left(q_1(t)\right)\left\{A_{1i}x_1(t)+B_{1i}u_1(t)+D_1h_1(t)\right\}\\ \dfrac{\partial p}{\partial V_{pv}}-0\end{bmatrix} \tag{39}$$

that can be written in the following form:

$$\dot{\bar{x}}_1(t)=\sum_{i=1}^{16}\mu_{1i}\left(q_1(t)\right)\left\{\bar{A}_{1i}x(t)+B_{1i}u_1(t)+\bar{D}_{1i}\bar{h}_1(t)\right\} \tag{40}$$

$$\text{where } \bar{A}_{1i}=\begin{bmatrix}A_1 & 0\\ C_{1i} & 0\end{bmatrix},\ \bar{B}_{1i}=\begin{bmatrix}B_{1i}\\ 0\end{bmatrix},\ \bar{D}_{1i}=\begin{bmatrix}D_1 & 0\\ 0 & -C_{1i}\end{bmatrix},\ \text{and } \bar{h}_1(t)=\begin{bmatrix}V_{pv} & u_c(t) & 0\end{bmatrix}^T \tag{41}$$

The boost control law is represented by the duty cycle u_1 described by:

$$u_1(t)=-\sum_{j=1}^{16}\mu_{1j}\,k_{1j}\,x_1(t) \tag{42}$$

with k_{1j} represent the controller gains corresponding to each sub-model.

Using the boost command law u_1, the PV-side system dynamic becomes in the following form:

$$\dot{\bar{x}}_1(t)=\sum_{i=1}^{16}\sum_{j=1}^{16}\mu_{1i}\left(q_1(t)\right)\mu_{1j}\left(q_1(t)\right)\left\{\left(\bar{A}_{1i}-\bar{B}_{1i}k_{1j}\right)\bar{x}_1(t)+\bar{D}_1\bar{h}_1(t)\right\} \tag{43}$$

5.2 Inverter Augmented System

$\bar{x}_2(t)$ represent the inverter augmented vector denoted as follows:

$$\bar{x}_2=\begin{bmatrix}x_2 & e_{2I}\end{bmatrix}^T \text{ with } \dot{\bar{x}}_2=\begin{bmatrix}\dot{x}_2 & e_2\end{bmatrix}^T \tag{44}$$

where $e_2(t)$ is the inverter error vector defined by:

$$e_2(t)=C_2\left(x_2(t)-x_{2r}(t)\right) \tag{45}$$

$$\text{with}\quad C_2=\begin{bmatrix}0 & 1 & 0\\ 0 & 0 & 1\end{bmatrix},\ e_{2I}=\int e_2 \text{ and } \dot{e}_{2I}=e_2 \tag{46}$$

Consequently, the inverter-augmented vector is described by the following expression:

$$\dot{\bar{x}}_2(t) = \begin{bmatrix} \sum_{i=1}^{8} \mu_{2i}\left(q_2(t)\right)\left\{A_{2i}x_2(t) + B_{2i}u_2(t) + D_2h_2(t)\right\} \\ C_2\left(x_2(t) - x_{2r}(t)\right) \end{bmatrix} \tag{47}$$

which can also be expressed in the form (48):

$$\dot{\bar{x}}_2(t) = \sum_{i=1}^{8} \mu_{2i}\left(q_2(t)\right)\left\{\bar{A}_{2i}x(t) + B_{2i}u_2(t) + \bar{D}_{2i}\bar{h}_2(t)\right\} \tag{48}$$

$$\bar{A}_{i2} = \begin{bmatrix} A_{2i} & 0 \\ C_2 & 0 \end{bmatrix}, \bar{B}_{2i} = \begin{bmatrix} B_{2i} \\ 0 \end{bmatrix}, \bar{D}_2 = \begin{bmatrix} D_2 & 0 \\ 0 & -C_2 \end{bmatrix}, \text{and } \bar{h}_2(t) = \begin{bmatrix} h_2^T & x_{2r}(t) \end{bmatrix}^T \tag{49}$$

Applying the following control law to this system:

$$u_2(t) = -\sum_{j=1}^{8} \mu_{2j}\, k_{2j}\, x_2(t) \tag{50}$$

where k_{2j} denotes the corresponding inverter controller gains to each sub-model.
The dynamic of the grid side system becomes in the form:

$$\dot{\bar{x}}_2(t) = \sum_{i=1}^{8}\sum_{j=1}^{8} \mu_{2i}\left(q_2(t)\right)\mu_{2j}\left(q_2(t)\right)\left\{\left(\bar{A}_{2i} - \bar{B}_{2i}k_{2j}\right)\bar{x}_2(t) + \bar{D}_2\bar{h}_2(t)\right\} \tag{51}$$

The boost-inverter controllers gains (k_{1j}, k_{2j}) previously denoted in the equations ((42), (50)) will be calculated using linear matrix inequality (LMI) resolution method (Sakthitharani, S., Sangeetha, R., Subha, S., & Deivamani, G., 2018; Kamal, E., & Aitouche, A., 2013), which will be described in the next section.

5.3 Stability Analysis

To ensure a good control for the systems, previously modeled, with a rejection of disturbance effects, the H_∞ criterion considered is given by:

$$\int_0^\infty e_{mI}^T e_{mI}\, dt < \delta^2 \int_0^\infty \bar{h}_m^T \bar{h}_m\, dt, \quad \delta > 0 \tag{52}$$

with $m = 1,2$; is the number of the treated system: PV-Boost system and the inverter-filter-network system.

The quadratic function of Lyapunov (Guisser, M., Abdelmounim, E., Aboulfath, M., & Medromi, H., 2014), which represents a tool for studying stability, is used to calculate the gains of the fuzzy controller. This function is expressed by:

$$V(\bar{x}_m) = \bar{x}_m^T P_m \bar{x}_m \tag{53}$$

where P_m is a symmetric positive definite matrix denoted by $P_m = P_m^T > 0$ and

$$\dot{V}(\bar{x}_m) = \dot{\bar{x}}_m^T P_m \bar{x}_m + \bar{x}_m^T P_m \dot{\bar{x}}_m < 0 \tag{54}$$

By these means, the stability condition will be given by:

$$\dot{V}(\bar{x}_m) + e_{mI}^T e_{mI} - \delta^2 \bar{h}_m^T \bar{h}_m < 0 \tag{55}$$

The first term development ($\dot{V}(\bar{x}_m) < 0$) gives the following inequality:

$$\begin{bmatrix} \left(\bar{A}_{mi}^T - k_{mj}^T \bar{B}_{mi}^T\right) P_m + P_m \left(\bar{A}_{mi} - \bar{B}_{mi} k_{mj}\right) & P_m \bar{D}_{mi} \\ \bar{D}_{mi}^T P_m & 0 \end{bmatrix} < 0 \tag{56}$$

To calculate the second term of the inequality (55), e_{mI} take the following form:

$$e_{mI} = F_{em} \bar{x}_m = F_{em} \begin{bmatrix} x_m \\ e_{mI} \end{bmatrix} \tag{57}$$

$$\text{where} \quad F_{e1} = \begin{bmatrix} 0 & 0 & 0 \\ 0 & 0 & 0 \\ 0 & 0 & 1 \end{bmatrix} \text{and } F_{e2} = \begin{bmatrix} 0 & 0 & 0 & 1 & 0 \\ 0 & 0 & 0 & 0 & 1 \end{bmatrix} \tag{58}$$

This allows to write the following expression:

$$\bar{x}_m^T F_{em}^T F_{em} \bar{x}_m - \delta^2 \bar{h}_m^T \bar{h}_m < 0 \tag{59}$$

whose matrix form is denoted by:

$$\begin{bmatrix} F_{em}^T F_{em} & 0 \\ 0 & -\delta^2 I_m \end{bmatrix} < 0 \tag{60}$$

By summing the two matrix terms (*56*) and (*60*), the inequality (55) becomes as follows:

$$\begin{bmatrix} \left(\bar{A}_{mi}^T - k_{mj}^T \bar{B}_{mi}^T\right) P_m + P_m \left(\bar{A}_{mi} - \bar{B}_{mi} k_{mj}\right) + F_{em}^T F_{em} & P_m \bar{D}_{mi} \\ \bar{D}_{mi}^T P_m & -\delta^2 I_m \end{bmatrix} < 0 \tag{61}$$

The multiplication on both sides by $\begin{bmatrix} P_m^{-1} & 0 \\ 0 & I_m \end{bmatrix}$ given the following forms:

$$\begin{bmatrix} P_m^{-1}\left(\overline{A}_{mi}^T - k_{mj}^T \overline{B}_{mi}^T\right) + \left(\overline{A}_{mi} - \overline{B}_{mi} k_{mj}\right) P_m^{-1} + P_m^{-1} F_{em}^T F_{em} P_m^{-1} & \overline{D}_{mi} \\ \overline{D}_{mi}^T & -\delta^2 I_m \end{bmatrix} < 0 \quad (62)$$

Putting $X_m = P_m^{-1}$ and $M_{mj} = k_{mj} P_m^{-1}$ and the substitution of these expressions in the previous equation given the following expression:

$$\begin{bmatrix} X_m \overline{A}_{mi}^T + \overline{A}_{mi} X_m - M_{mj}^T \overline{B}_{mi}^T - \overline{B}_{mi} M_{mj} + X_m F_{em}^T F_{em} X_m & \overline{D}_{mi} \\ \overline{D}_{mi}^T & -\delta^2 I_m \end{bmatrix} < 0 \quad (63)$$

The Schur complement lemma application, given:

$$\begin{bmatrix} X_m \overline{A}_{mi}^T + \overline{A}_{mi} X_m - M_{mj}^T \overline{B}_{mi}^T - \overline{B}_{mi} M_{mj} & X_m F_{em}^T & \overline{D}_{mi} \\ F_{em} X_m & -I_m & 0 \\ \overline{D}_{mi}^T & 0 & -\delta^2 I_m \end{bmatrix} < 0 \quad (64)$$

The resolution of this matrix inequality allows to deduce the fuzzy controllers' gains $k_{mj} = M_{mj} X_m^{-1}$.

By replacing the gains k_{1j} in the expression (42), by their values calculated with the first LMI, and using the PWM (Figure 2), the boost converter cyclic ratio u_1 is calculated, allowing the PVG to operate at its maximum power.

After that, the PWM application to the gains k_{2j}, deduced from the second LMI resolution, allows to calculate the command laws of the inverter using the equation (50).

6.0 SIMULATION RESULTS

The proposed system is designed to transfer the maximum power generated by the PV panel into the utility grid whatever the meteorological data changes. The photovoltaic array is arranged in two parallel strings with 555 cells in each string.

Using climatic variations represented in table 3, the DC variables in the PV-side are firstly represented in Figure 5.

Table 3. Climatic variations

Time (s)	0	2	3	4	5	10
G (w/m2)	600	700	800	900	800	700
T (°C)	24	25	26	27	26	25

The curve (5.a) proves that the PV panel voltage is approximately equal to the optimal voltage (V_{pv-opt}) which depends on the climatic variations. The PVG generated current and power varies with the temperature and sunshine changes.

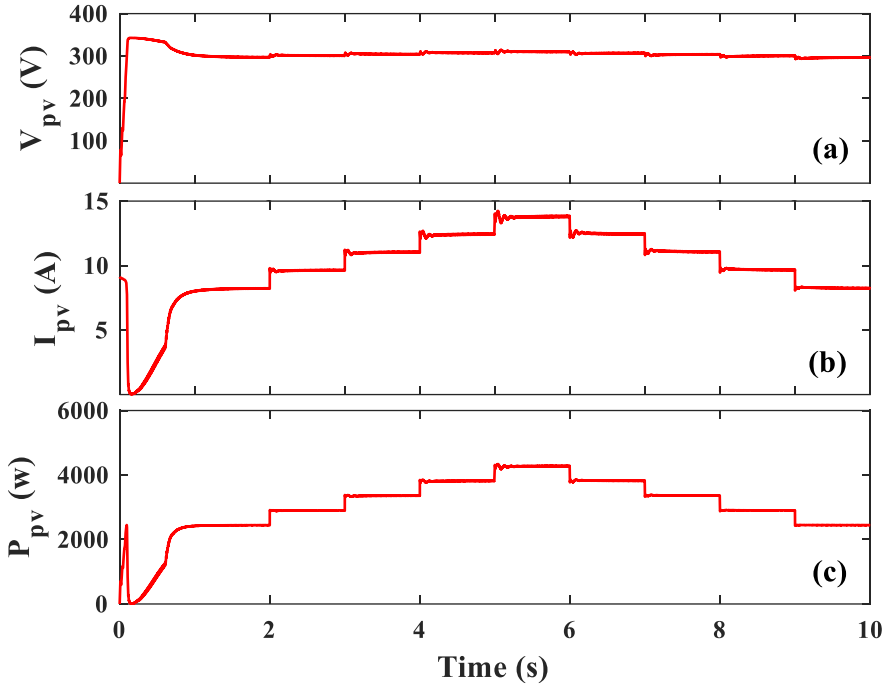

Figure 5. Photovoltaic components:
(a) Voltage, (b) Current and (c) Power

In addition, the duty cycle curve represented in Figure 6. (a), calculated with the first controller to control the Boost transistor, follows the climatic variations allowing to vary the voltage of the PV generator in order to extract the maximum power.

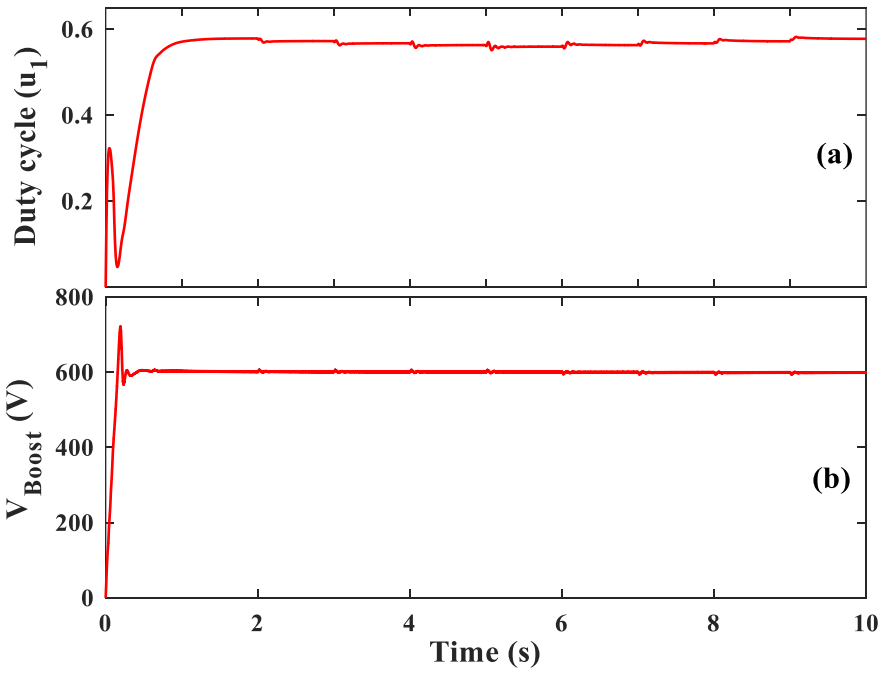

Figure 6. Duty cycle and Boosted voltage

The boost converter is used to increase the input voltage and produce the boosted voltage represented in the curve (b) of Figure. 6.

The Ipv-Vpv and Ppv-Vpv panel characteristics are also given in the Figure 7 and Figure 8 to better validate and demonstrate the T-S MPPT method performance. This algorithm allows to command the boost converter in order to track the maximum power point produced by the panel.

The two following curves show the capacity and effectiveness of the developed algorithm to follow the MPP whatever the environmental changes.

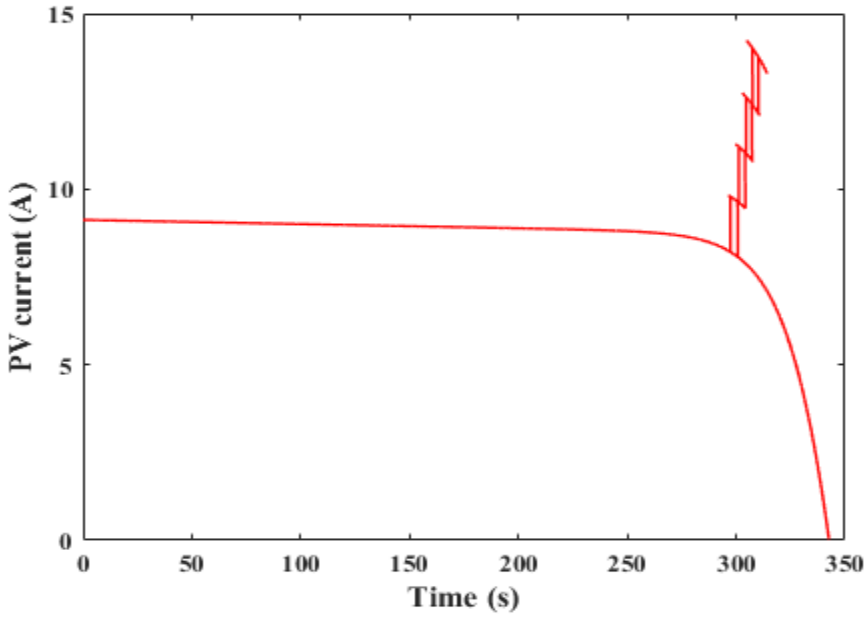

Figure 7. Current-Voltage panel characteristic

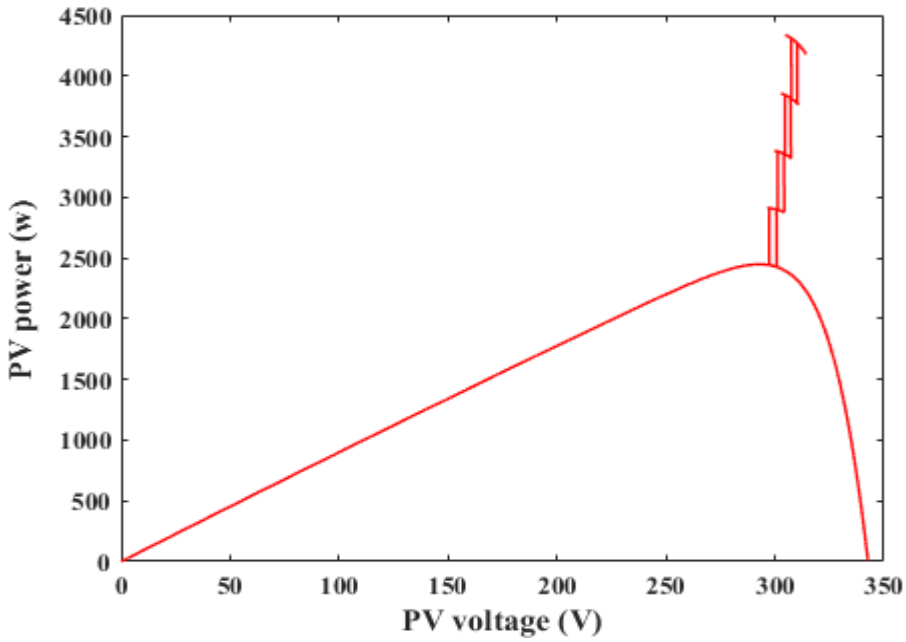

Figure 8. Power-Voltage panel characteristic

In the second part, the inverter command laws (Figure 9) calculated with the second T-S controller are represented in the Figure 9 in order to show their variations with the climatic fluctuations.

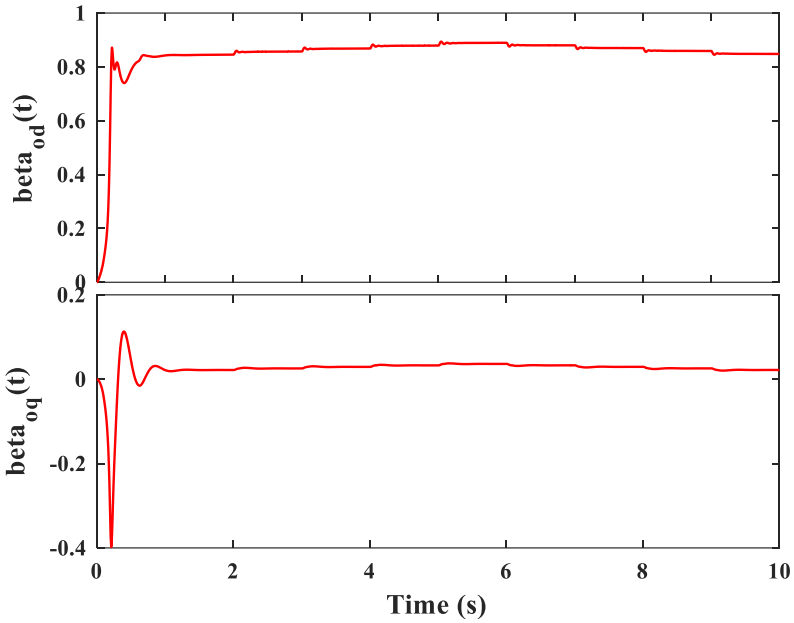

Figure 9. Inverter command laws

Next, the d-q inverter output currents are shown in the Figure 10. It is clear that the quadratic current follows the specified reference value ($i_{oqRef} = 0$), whereas the direct component follows the climatic conversion. The same can be observed in Figure 11 for the quadratic and direct voltage of the inverter and the electrical network.

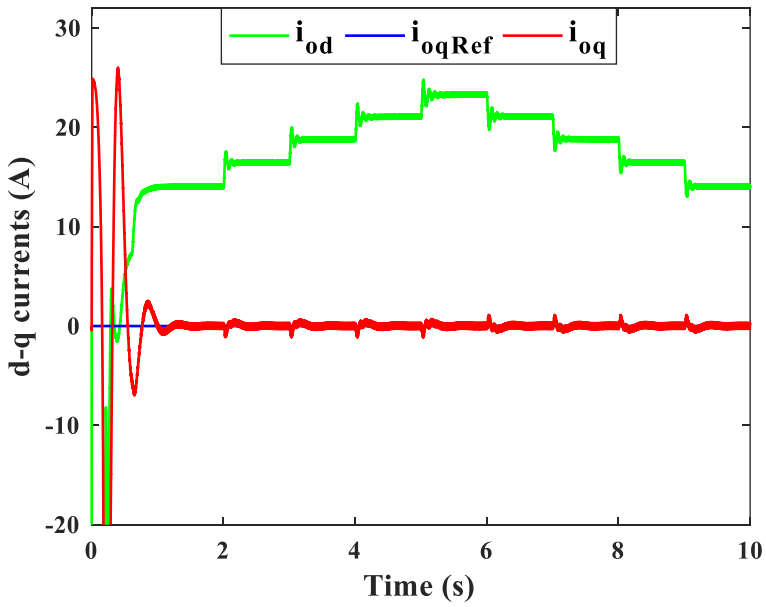

Figure 10. Direct-Quadratic currents (A)

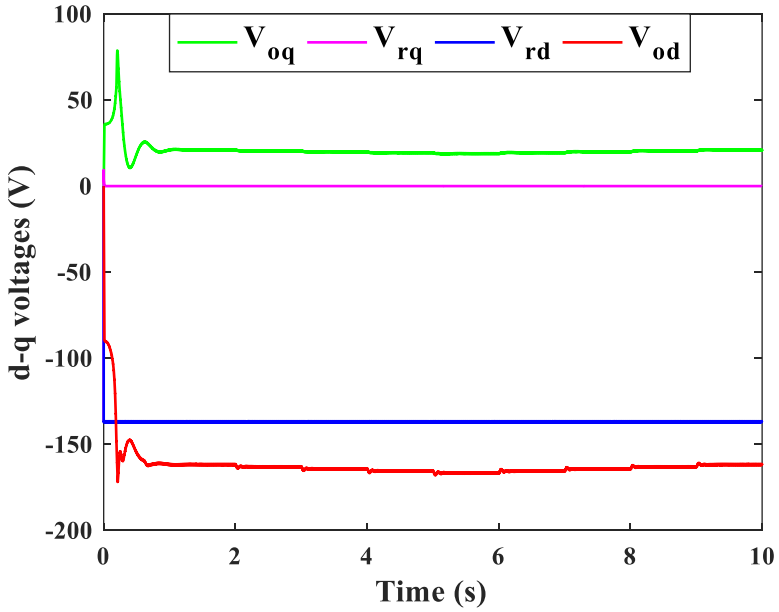

Figure 11. Direct-Quadratic voltages of inverter-grid (A)

To verify the alternative form of the currents and the voltages of each phase transformed with the inverter, the sine waveforms of the inverter current-voltage outputs are represented by Figure 12 and Figure 13.

As soon as the phase inverter voltage reaches the phase network voltage value, climatic fluctuations effects will be negligible on this signal, whereas the dynamic values of the phase currents vary with these fluctuations.

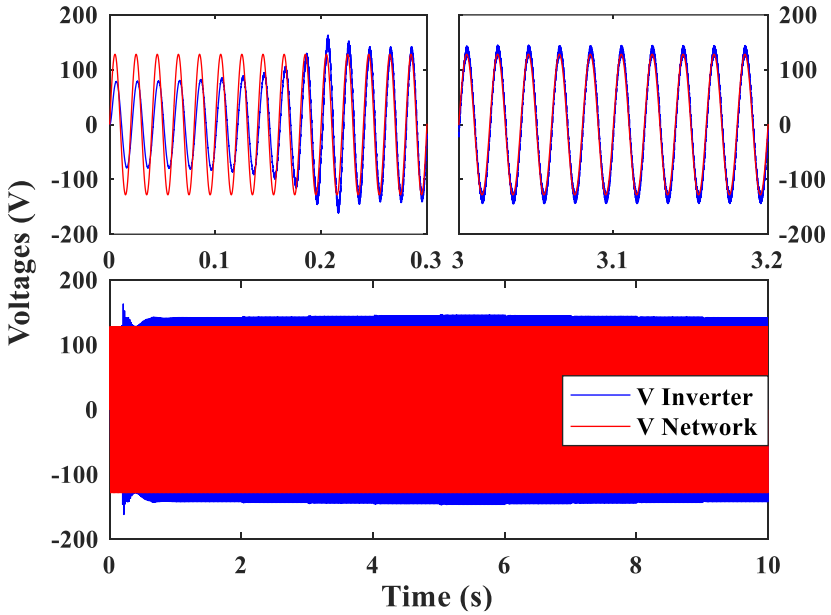

Figure 12. Sine waveform of phase voltages of the inverter and network

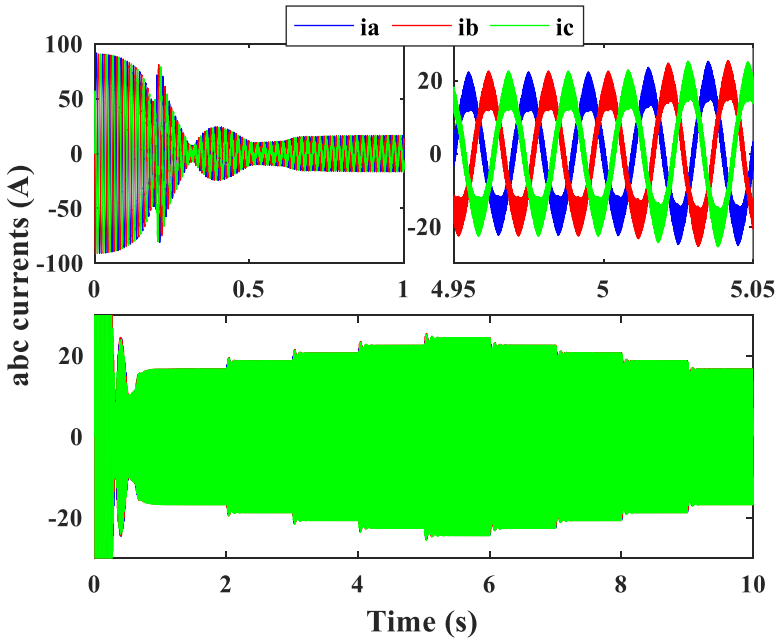

Figure 13: Sine waveform of phase currents

7.0 CONCLUSION

In this work, a robust controller based on the Fuzzy Takagi-Sugeno (T-S) technique is used to extract and transfer the maximum power of the photovoltaic system to the electrical grid. This method makes it possible to determine, in the first step and using a T-S controller, the duty ratio of the DC-DC converter in order to optimize the extraction of photovoltaic energy whatever the atmospheric variations. In the next step, a second T-S controller is also used to control the DC-AC inverter switchers' in order to transfer the optimal energy supplied by the PV array to the utility grid while regulating the DC bus voltage and canceling the reactive power. To reduce the harmonics and improve the quality of the electrical power injected to the network, a PWM and a R-L filter are used. The simulation results' analysis and interpretation, under MATLAB environment, prove the controlled system' robustness and performance using the two fuzzy T-S controllers. Whatever the climatic fluctuation, these results attest that the used controllers allow the optimal power fast extraction and the active power injection into the network.

REFERENCES

Refaat, A., Kalas, A., Daoud, A., & Bendary, F., (2013). A Control Methodology of Three Phase Grid Connected PV System. *Power Systems Conference*.

Abada, S., & Lehuy, H., (2011). *Etude et Optimisation d'un Générateur Photovoltaïque pour la Recharge d'une Batterie avec un Convertisseur SEPIC*. (Master dissertation). Semantic Scholar.

Afkar, H., Shamsinejad, M. A., & Ebadian, M., (2016). A Grid-Connected PV, Inverter with Compensation of Load Active and Reactive Power Imbalance for distribution Networks. *Iranian Journal of Electrical & Electronic Engineering*, 12(2):168-176.

Ajaamoum, M., Kourchi, M., Bouachrine, B., & Ihlal, A., & Bouhouch, L., (2015). Comparison of Takagi-Sugeno fuzzy controller and the command "P & O" for extracting the maximum power from a photovoltaic system. *Innovative Space of Scientific Research Journals*, 10(1):192-206.

Akoro, E., Amadou, S. M., & Jean-Philippe, T. G., F., (2017). Differents topologies of three-phase grid connected inverter for photovoltaic systems, a review. *Revue du CAMES – Sciences Appliquées et de l'Ingénieur*, 2(2):33-41.

Belattar, A., Chennanni, M., & Doubabi, S., (2015). TS Fuzzy Output Control for a Boost Converter in PV Systems. *3rd International Renewable and Sustainable Energy Conference (IRSEC)*, 1-6.

Bouhafs, A. Lokmane, B. M., & Mohamed, D., (2015). Grid connected photovoltaic system, for a 800 W. *ScienceDirect Journal of Elsevier Energy Procedia*, 74:414-422.

Cen, Z., (2017). Modeling and Simulation for an 8 kW Three-Phase Grid-Connected Photo-Voltaic Power System. *De Gruyter Open Central European Journal of Physics*, 15(1):603-612.

Cheng, P. C., Peng, B. R., Liu, Y. H., Cheng, Y. S., & Huang, J. W., (2015). Optimization of a Fuzzy-Logic-Control-Based MPPT Algorithm Using the Particle Swarm Optimization Technique. *Open Access Journal Energies*, 8(6):5338-5360.

Chiu, C. S., (2010). T-S Fuzzy Maximum Power Point Tracking Control of Solar Power Generation Systems. *IEEE Transactions on Energy Conversion*, 25(4):1123-1132.

Eugineraj, K., & Uma, G., (2013). T-S Fuzzy Maximum Power Point Tracking Modelling And Control Of Solar Power Generation. *International Journal of Engineering Research and Applications (IJERA)*, 3(1):1887-1892.

Guisser, M., Abdelmounim, E., Aboulfath, M., & Medromi, H., (2014). Nonlinear Control Design for Maximum Power Point Tracking and Unity Power Factor of a Grid-Connected Photovoltaic Renewable Energy Systems. *IOSR Journal of Electronics and Communication Engineering (IOSR-JECE)*, 9(5):62-71.

Gupta, S., Garg, R., & Singh, A., (2015). TS-Fuzzy Based Controller for Grid Connected PV System. *IEEE India Conference (INDICON)*, 23, 1-6.

Hamrouni, N., Jraidi, M., Dhouib, A., & Cherif, A., (2017). Design of a command scheme for grid connected PV systems using classical controllers. *ScienceDirect Journal of Elsevier Electric Power Systems Research*, 143:503-512.

Kamal, E., & Aitouche, A., (2013). Design of Maximum Power Fuzzy Controller for PV Systems Based on the LMI-Based Stability. *Springer Advances in Intelligent Systems and Computing*, 230:77-78.

Kouro, J., Leon, I. J., Vinnikov, D., & Franquelo, G. L., (2015). Grid-Connected Photovoltaic Systems: An Overview of Recent Research and Emerging PV Converter Technology. *IEEE Industrial Electronics Magazine*, 9(1):47-61.

Kumar, A., Vempati, S. A., & Behera, L., A. V., (2013). T-S Fuzzy Model Based Maximum Power Point Tracking Control of Photovoltaic System. *IEEE International Conference on Fuzzy Systems (FUZZ-IEEE)*, 1-8.

Mahfouz, M. M., (2015). On-Line Maximum Power Point Tracking for Photovoltaic System Grid Connected Through DC-DC Boost Converter and Three Phase Inverter. *Journal of Fundamentals of Renewable Energy and Applications*, 5(4):1-5.

Ounnas, D., Ramdani, M., & Chenikher, S., & Bouktir, T., (2017). An Efficient Maximum Power Point Tracking Controller for Photovoltaic Systems Using Takagi–Sugeno Fuzzy Models. *Arabian Journal for Science and Engineering*, 42(12):4971–4982.

Rana, M. M., Ali, R. M., Ajad, A. K., & Moznuzzaman, M., (2016). Analysis of P&O and INC MPPT Techniques for PV Array Using MATLAB. IOSR *Journal of Electrical and Electronics Engineering (IOSR-JEEE)*, 11(4):80-86.

Sakthitharani, S., Sangeetha, R., Subha, S., & Deivamani, G., (2018). Power quality improvement in solar by using fuzzy logic controller. *International Research Journal of Engineering and Technology (IRJET)*, 5(4):1164-1169.

Salah, C. B., & Ouali, M., (2011). Comparison of fuzzy logic and neural network in maximum power point tracker for PV systems. *ScienceDirect Journal Elsevier Electric Power Systems Research*, 81(1):43-50.

Sekhar, P. C., & Mishra, S., (2014). Takagi–Sugeno fuzzy-based incremental conductance algorithm for maximum power point tracking of a photovoltaic generating system. *IEEE IET Renewable Power Generation*, 8(8):900-914.

Srivastava, M., & Saxena, A., (2016). Direct and Quadrature Axis V oltage and Current Control of a Three Phase Grid Connected PV System with Adaptive Fuzzy Logic MPPT Controller. *IEEE International Conference on Power Electronics. Intelligent Control and Energy Systems (ICPEICES)*, 1-5.

Yahya, A. O. M., Mahmoud, A. O., & Issakha, Y., (2008). Etude et modélisation d'un générateur photovoltaïque. *Review of Renewable Energies*, 11(3):473 – 483.

Yuanlong, L., & Ji, Z., (2008). An Approach on T-S Fuzzy Model and Control of Buck-boost Converter. *Proceedings of the 7th World Congress on Intelligent Control and Automation*, 91-96.